Characterizing tribological behavior of fresh concrete against formwork surfaces

N. Spitz, N. Coniglio, Laurent Libessart, M. El Mansori, Chafika C. Djelal Djelal

Characterizing Tribological Behavior of Fresh Concrete Against Formwork Surfaces

N. Spitz[1], N. Coniglio[1], L. Libessart[2], M. El Mansori[1,3], C. Djelal[2]

[1]Arts et Métiers ParisTech d'Aix-en-Provence, Laboratory of Mechanics, Surface and Materials Processing (MSMP-EA7350), 2 cours des Arts et Métiers, 13617 Aix-en-Provence – France

[2]Univ.Artois, ULR 4515, Laboratoire de Génie Civil et géo-Environnement (LGCgE), F-62400 Béthune, France

[3] Texas A&M Engineering Experiment Station, College Station, TX 77843, USA

A. Abstract

The friction of concrete on the interior skin of formworks takes place during the pouring of concrete into the molds. The present work investigates the friction of a granular material (i.e. fresh concrete) against metallic and polymeric surfaces. Interfacial behavior between different formulated concretes and formwork skins is characterized using a plane-plane tribometer dedicated to concrete tribometer. The formwork surface is measured before and after testing to quantify the wear issue. A Coulomb friction law is observed within the range of tested normal pressures. Tribological tests reveal that friction mechanisms depend on the interface properties. Two underlying mechanisms are hypothesized to explain the wearing of the formwork skin: a granulate-formwork solid-solid friction and a capillary-dominated friction.

B. INTRODUCTION

In the construction industry, the majority of reinforced concrete walls are constructed today using shuttering to hold the concrete while curing. Filling correctly the formwork with concrete requires the knowledge of several properties, including the characteristics of the concrete / formwork interface.

The friction generated by the concrete against the skin acts favorably by lowering the normal pressure of the concrete against the formwork [1][2] and subsequently reducing the dimensioning of the formwork [3][4][5][6][7]. When performing tribological tests, choices about the operating conditions must be made (test variables to be measured, parameters to be varied, definition of a tribometer) [8]. The literature that has been devoted up to now to concrete tribology is poor and is almost oriented towards volume rheology [9][10][11]. Fresh concrete is a non-Newtonian material, sometimes threshold and often thixotropic [12][13], with a Binghamian behavior [14]. Its steady state behavior has been defined using a pseudo-plastic or a Herschel-Bulkley model [15][16][17].

Many devices have been developed to study the tribological behavior of fresh concrete against a solid surface [18][19][20][21][22][23]. The first civil engineering tribometer designed by Djelal [24] was used

to study the friction between the clay paste and the wall. Its plane / plane principle was developed successively by Beaumel [25] to study the extrusion of clay / sand / water mixtures under industrial conditions and later by Vanhove et al. [5] to study on fresh concrete-plane coupon interface the influence of parameters such as the concrete formulation [3][2][18][26], the plate roughness [27][28], the sliding speed [1][27][28][18][29][30], the normal pressure [1][27][28][30], and the nature of the formwork oils [2][31][29][5][32][33].

Different empirical models exist between the normal pressure and the frictional stress at the concrete-formwork interface [28][1][34]. These models are mostly limited to small normal pressures that avoid granular behavior at the interface. Some models are based on Janssen's theory of silos [35][36][37]. Others considered a simple Coulomb's law that is valid for the friction between a wall and granular materials such as powders, dry sand or solids, expressing the proportionality between the tangential and normal stresses of contact. A Coulomb-type of friction is applicable to fresh concrete within a limited range of normal pressures (50-150 kPa) [30][2][3][31][26][29] corresponding to the commonly used formwork heights (2 to 6 meters). The increase in pressure leads to a migration of fines towards the boundary layer until the high compression of the concrete displaces the boundary layer from the surface of the skin to the inside of the concrete [1][27][30]. Friction and wear at the concrete-formwork interfaces are related to the compactness of the granular skeleton and the fines content in the mixture [27][33]. The tangential friction combined with the abrasiveness of concrete cause significant wear problems on the surface of the formwork [27] which lead to a modification of the topography of the wall surface and aesthetic defects on the surface of the concrete wall [28]. Knowledge of the tribological characteristics of the fresh concrete on formworks is in conclusion important to prolong the lifespan of the formwork.

The surface topography and roughness of the formwork influence both the static interactions [38][39][40][41] and the tribological behavior [1][27] with fresh concrete through interactions with the fines and granulates of the concrete. At normal pressures smaller than 140 kPa, the boundary layer is mainly composed of water and fines. This layer is sheared during the relative movement of the concrete leading to a negligible influence of the roughness of the formwork on the frictional behavior [30]. However, above a threshold normal pressure of 140 kPa, it is assumed that the liquid phase initially trapped at the interface migrates inside the sample under the effect of pressure. The concrete / formwork friction is dominated by a granular behavior where the coarser aggregates are mechanically anchored in the asperities of the formwork surface [30][5]. Therefore, at high normal pressures, greater roughness of the formwork surface significantly increases the frictional interaction with fresh concrete. The frictional stress is minimized when the diameter of the particles is equal to the roughness of the substrate [24]. Unfortunately, this finding is difficult to apply in the construction industry because concrete contains a wide range of particle sizes from micrometer to centimeter scales.

The present research paper investigates the effect of the functional signatures of the formwork surfaces on the concrete friction. Using a tribometer developed specifically for fresh concrete, the friction coefficient was determined for different formwork surfaces and concrete formulations. The influence of surface condition, surface roughness, and contact pressure on the friction phenomena is discussed. Interfacial friction mechanisms are identified and discussed.

C. EXPERIMENTAL

I. Tribological testing

Friction and wear properties were studied by means of a portable version of a plane-plane tribometer initially developed by Djelal for clay [24] and successfully used for tribological campaigns on fresh concrete [1][27][18]. The aim is to simulate the casting of the concrete inside the formwork on construction sites. The concrete speed and pressure along the formworks are simulated by the translation speed of the skin and the loading of the concrete, respectively.

The tribological testing device is designed to generate friction of fresh concrete on a plane coupon under controlled conditions (Figure 1). The fresh concrete is held stationary while the plane coupon slides at a constant displacement rate in-between two cylinders containing fresh concrete to create a relative shear movement at the coupon-concrete interface. The effect of gravity is neglected since the plate moves horizontally. The tribological test fixture preloads the concrete on the coupon. This is accomplished by placing the fresh concrete in two 120 mm-diameter cylindrical sample holders and pushing it at a predefined normal pressure against the plane coupon. The pressure is exerted by a pneumatic jack then transmitted to the concrete by a piston connected to the movable bottom of the specimen holders. The motor coupled to a worm screw allows the sliding of the metal plate against the fresh concrete.

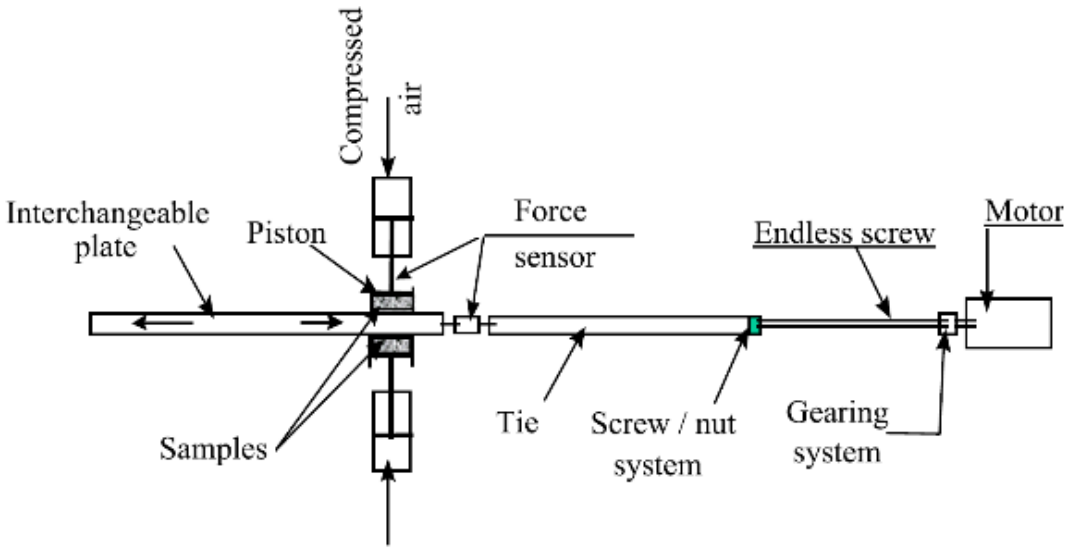

Figure 1. Overview of tribological test with superimposed captures of test progress [27].

The test sequence consisted of the following steps:

(i) Clamp test coupon into tribological test frame
(ii) Apply given preload
(iii) Measure friction induced without fresh concrete
(iv) Cast fresh concrete in holders and preload piston
(v) Displace test coupon at constant rate and measure tangential force

(vi) Remove test coupon for wear quantification

II. Operating variables

Tests were made on plane coupons in contact with fresh concrete by varying its operating parameters. The concrete contact pressures taken into account are 60, 80 and 110 kPa which correspond to the lateral pressures exercised by the concrete on formworks of 2.4, 3.2, and 4.4 m in height. The maximum pressure of 110 kPa was selected as previous works demonstrated a migration of the boundary layer towards the inside of the fresh concrete for pressures above 140 kPa [18][33][30]. A single sliding speed of 0.83 mm.s^{-1} was selected corresponding to a concrete placing speed of 3 m.h^{-1}. The displacement rate was kept constant as the friction coefficient is constant for small sliding speeds [28]. The repeatability of tribological test results was examined by performing three times each fixed condition.

III. Tangential force measurement

The displacement of the test coupon resulted at the concrete-coupon interface in a tangential friction force that is opposed to the displacement. For each test, the tangential (or frictional) force F_{mes} that hinders the transverse movement of the plate was measured with a force cell (load capacity of 17 kN) and is the sum of two friction components: a parasitic friction force generated by the watertight sealing system of the sample holders (F_v) and a friction force induced by the fresh concrete in contact with each of the two faces of the coupon ($2.F_b$) considering the symmetry of the system:

$$F_{mes} = F_v + 2.F_b \quad \text{(Eq. 1)}$$

F_v is measured by displacing the plane coupon without concrete prior to each test. The interaction of the coupon with fresh concrete is thus given by:

$$F_b = \frac{F_{mes} - F_v}{2} \quad \text{(Eq. 2)}$$

The frictional stress τ_b of the concrete on the coupon is calculated by dividing the friction force F_b with the surface of the coupon in contact with the concrete S_c according to:

$$\tau_b = \frac{F_b}{S_c} = \frac{F_b}{\frac{\pi.d^2}{4}} \quad \text{(Eq. 3)}$$

where the holder has a diameter d of 120 mm.

IV. Formwork plates

Three formwork surfaces commonly used for the building of concrete walls were studied in this work: two metallic substrates (PMr1 and PMr2) and an adhesive polymeric coating (RPa1) applied on a metallic substrate. Plane plates of 180 x 474 mm² were cut from 2000 x 1000 x 5 mm laminated plates using the laser beam cutting process.

Analyzes of the skin materials are detailed in previous works [39][40][41]. PMr1 is a steel with controlled oxide layers consisting of a non-uniform 11.4 µm-thick oxides layer with a Fe_3O_4 bottom

sub-layer and a α-Fe_2O_3 top sub-layer as shown in Figure 2. The Fe_2O_3 layer is known to be hard and wear resistant [42][43][44][45][46][39]. PMr2 is a high strength, corrosion resistance iron-based alloy with no specific surface layer. The composition of the commercial coating RPa1 was a composite material at PP-grafted-anhydride matrix with about 12-15% of alumina filler, in agreement with patent WO 2016/059193 A1. Optical observations revealed three sub-layers composing the polymeric formwork coating (Figure 3): a 145 µm-thick adhesive layer, a 420 µm thick control layer, and a 160 µm-thick PP functional layer in contact with the concrete.

Figure 2. Cross-section of PMr1 specimen

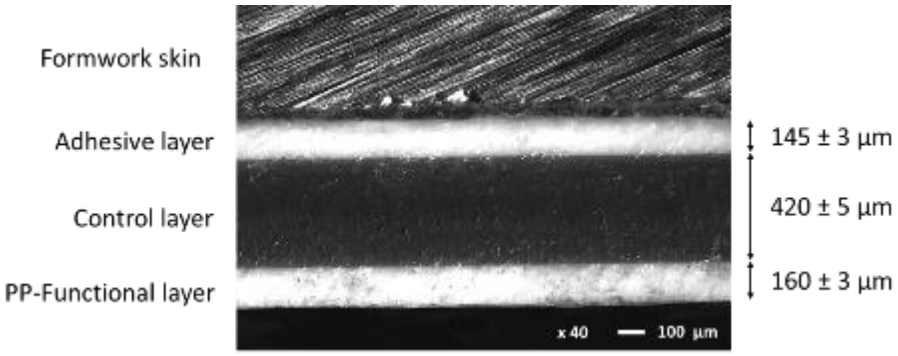

Figure 3. Cross-section of RPa1 specimen

V. Concrete formulations

Two concrete formulations were investigated as shown in Table 1. The first concrete (C1) is a conventional concrete without additive. The second concrete (C2) is a self-compacting concrete much more fluid due to the superplasticizer (SP) addition. Limestone filler was added to the cement to form the binder.

Table 1. Concrete formulation

	C1	C2
Paste volume (%)	32	36
Cement CEM I 52,5 CE CP2 NF ($kg.m^{-3}$)	265	350
Limestone filler BETOCARB-MQ ($kg.m^{-3}$)	28	133
Sand 0/4 ($kg.m^{-3}$)	792	789
Crushed aggregate 4/8 ($kg.m^{-3}$)	271	-
Crushed aggregate 6/20 ($kg.m^{-3}$)	734	-
Crushed aggregate 4/12.5 ($kg.m^{-3}$)	-	822
Superplasticizer Viscocrete Tempo 9 (L)	-	3.3
Water (L)	201	181
Water/binder ratio	0.57	0.37

The concrete is similar to the one used in previous works [3][2][27][28][33][29][30][31]. The cement characterized by the laser diffraction technique has a maximum grain size of 60 µm with a majority of grains of 20 µm diameters (3.4% of the grains) and 80% of the particles smaller than 20 µm in diameter (Figure 4). The maximum grain diameter of limestone filler is 80 µm. The granulometry of crushed aggregates and sand are drawn according to the weight percent passing each sieve size (Figure 5) according to the standard NF EN 933.

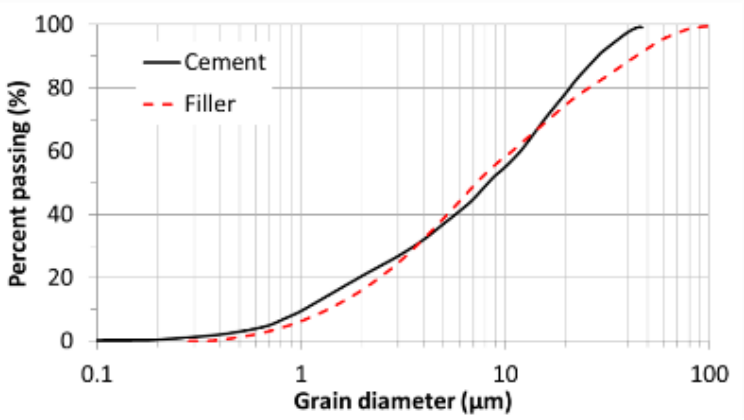

Figure 4. Size distribution of cement and filler measured by laser diffraction analysis.

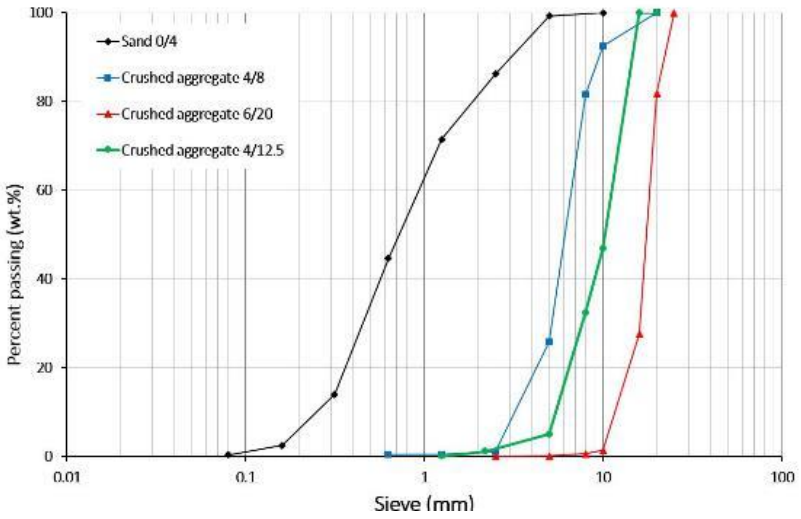

Figure 5. Size distribution of sand and crushed measured according to NF EN 933 .

The mixing mode of concretes was defined according to standard NF P 18-404 [47] and the procedure applied is shown in Figure 6. In the case of C2, the superplasticizer is added simultaneously with $\frac{2}{3}$ of remaining water. The 10-minutes stop allows the aggregates, especially sand, to absorb the injected water. A concrete batch of 0.02 m^3 was prepared for each tribological test.

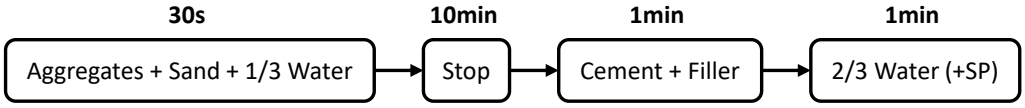

Figure 6. Mixing procedure of concretes with indicated duration for each step.

In order to check the conformity of concretes, the workability in the fresh state is measured by a slump flow test. These tests are carried out using an Abrams cone according to the NF EN 12350 standard series [48]. The slump or the spreading values are directly related to a class of concrete according to standard NF EN 206 [49]. For the conventional concrete C1, the desired concrete class was S3, namely slumps between 12 and 14 cm. These values indicate a very viscous concrete. For the self-compacting concrete C2, the mean spread was 700 ± 15 mm (SF2 category) which is the most common category for building vertical walls.

The flow stress indicates the freedom of relative movement of the grains. The flow stress τ_0 of C1 was estimated by using the formula for normal concrete:

$$\tau_0 = \frac{\rho}{34.7}(30 - s) + 212 \qquad \text{(Eq. 4)}$$

, where ρ is the concrete density (2350 $kg.m^{-3}$) and s the value of the Slump cone (12-14 cm). The τ_0 value obtained with Eq. 4 for C1 is between 1295 and 1431 Pa.

The flow stress τ_0 of C2 was estimated by using the formula for self-compacting concrete:

$$\tau_0 = \frac{\rho.g}{11740}(808 - s) \quad \text{(Eq. 5)}$$

, where ρ is the concrete density (2350 kg.m^{-3}), s the value of the Abraham cone (685-715 mm), and g the gravitational constant (9.81 m.s^{-2}). The τ_0 value obtained with Eq. 5 for C2 is between 182 and 241 Pa.

The smaller flow (or yield) stress for C2 indicates a freer movement of the grains. This is due in part to the deflocculating action of the superplasticizer which scatters the cement grains by the steric effect and electrostatic repulsion [26].

VI. Wear quantification

The surface geometry is significantly altered during casting by the concrete movement against the formworks, especially for non-lubricated surfaces. Surface topography is a factor that significantly affects the performance of formworks [40,41,50]. This factor is used in this research study to probe and quantify the wear of formwork plates. The surface topography was measured using a white-light interferometry microscope (WLIM) VEECO NT3300 over a 8x8 mm² area. The surface was sampled at 4121 x 4121 points with a 1.9 µm step scale along X- and Y-directions. This step is smaller than more than 80% of the diameter of the fines included in the concrete. A multi-scale characterization of the surfaces was preliminary performed in order to determine a relevant measurement scale [51]. Surface roughness profiles were sampled in frequency components from 3.10^{-2} to 8 mm^{-1} using the decomposition approach of continuous wavelets [52]. Above a scale of 1 mm, the surfaces showed fractal domains. Therefore, in an aim of obtaining representative data acquired in a small duration time, areas of 8x8 mm² were chosen.

The arithmetic mean height (S_a), the developed interfacial area ratio (S_{dr}), the peak material volume (V_{mp}), the core void volume (V_{vc}) and the valley void volume (V_{vv}) were computed according to the norm ISO 25178-2 [53]. V_{mp}, V_{vc} and V_{vv} are calculated from 0 to 10 %, 10 to 80 % and 80 to 100 % of the bearing ratio, respectively [54]. The topographical analyses have been carried out on each tested plate before and after the tribological tests to quantify the degradation caused by the friction of the concrete. The analyzed zones on the plates after the tests were chosen according to their strong degradation due to the concrete friction. Both sides of the plate were characterized, and the average of the roughness values was retained because no significant difference between the two sides of the plate was noticed. Formwork surfaces were analyzed after cleaning with water and alcohol to remove traces of residual concrete.

D. EXPERIMENTAL RESULTS

I. Characterization of skin surface prior to testing

The topography was mapped using interferometry measurements over a 8x8 mm² area (Figure 7) from which roughness values were calculated. Several parameters have been considered to characterize the surfaces in regard to their friction behavior. The parameters S_a and S_q are associated to the ability

to trap the cement particles at their surface. The parameter S_{dr} expresses the true surface of contact between the substrate and the concrete. The parameters V_{vc} and V_{vv} correlate to the quantity of particles of cement trapped in the asperities. Finally, the parameter V_{mp} is linked to the properties of friction and wear of the formworks.

The values of S_a, S_{dr}, V_{vc} and V_{vv} are presented in Table 2 for each skin surface prior to testing. The surface PMr1 contains many micro-asperities that are correlated to small S_a (0.9µm) and S_{dr} (2.4%) values. The surface PMr2 is constituted of large plateaus that explain the high S_a (3.3 µm) and S_{dr} (11.9%) values. The surface RPa1 is constituted of numerous high peaks leading also to high S_a (2.5 µm) and S_{dr} (8.2%) values. The highest are the roughness values, the greater susceptibility the particles can be trapped in the surface asperities. This trapping ability is enhanced by the higher V_{vc} than V_{vv} values.

Table 2. Roughness parameters of formwork skins before concrete friction

Roughness parameters	PMr1	PMr2	RPa1
S_a (µm)	0.9 ± 0.1	3.3 ± 0.2	2.5 ± 0.4
S_{dr} (%)	2.4 ± 0.2	11.9 ± 1.6	8.2 ± 1.6
V_{mp} ($nm^3.nm^{-2}$)	50 ± 10	70 ± 20	80 ± 10
V_{vc} ($\mu m^3.\mu m^{-2}$)	170 ± 10	410 ± 20	230 ± 30
V_{vv} ($nm^3.nm^{-2}$)	150 ± 20	510 ± 30	210 ± 30

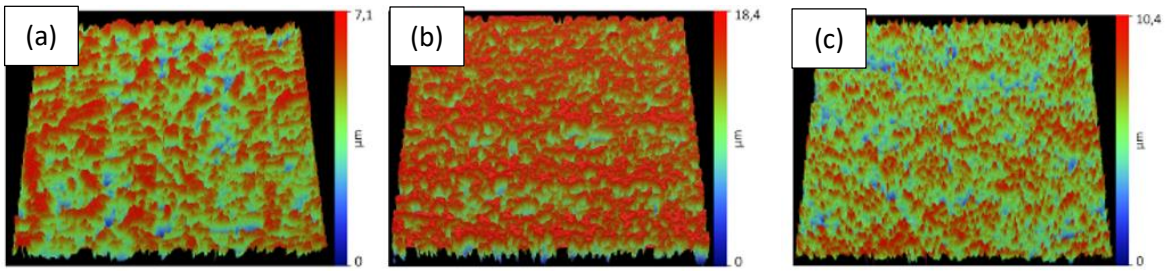

Figure 7. Topographies of surfaces tested prior to friction: (a) PMr1, (b) PMr2, and (c) RPa1.

II. Friction force measurement

An example of tangential force measurement made during the tribological test is presented in Figure 8, highlighting the variation in parasitic force (F_v) and total force (F_{mes}) with time. The F_v curve corresponds to the variations in the parasitic force without fresh concrete and is measured prior to each test. F_v varies from 9 to 16 daN and represents 25 to 38% of the total measured force F_{mes}.

At the start, a strong increase in F_{mes} measurements leads to a maximum force value that corresponds to the static friction force. A delay of a few seconds, corresponding to a displacement of several millimeters, is necessary to exceed the static friction force and eliminate some backlash. It is followed by a steady regime during which the dynamic friction force is constant. No difference is measured between static and dynamic friction. Similar observations have been made in other works for testing

conditions involving a concrete directly put in contact on a plate prior to tribological testing and without the application of a release agent that induces the formation of emulsion and soap at the interface [24][27][29][55].

The tangential forces F_v and F_{mes} are obtained by averaging the plateau during the steady regime. The repeatability of the tribological test was examined for each single test condition. Performing the tribological test three times for each fixed condition resulted in an average variation in measured friction stress of ± 2 kPa demonstrating good repeatability within 20 %.

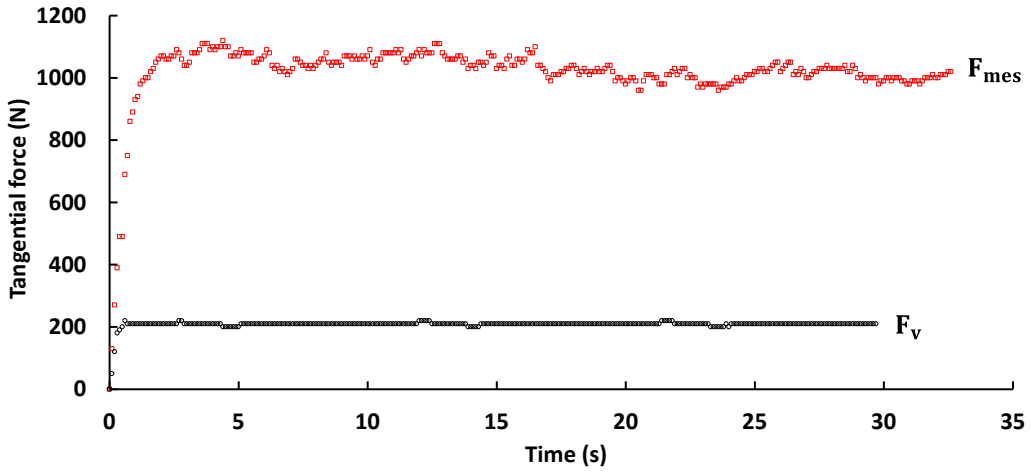

Figure 8. Temporal evolution in tangential force for PMr2 plate with C1 concrete pressured at 110kPa.

III. Wear surface ranking

A first qualitative ranking was performed from visual observation after the tribological test. Undamaged and highly damaged specimens were ranked from 1 to 5, respectively, as shown in Table 3. The total rating indicates the overall wear resistance of the specimens. Both C1 and C2 concrete compositions generate deeper scratches as the pressure increases. The RPa1 surface is always more damaged than PMr1 that is in turn more damaged than PMr2.

The ranking of wear resistance when using the concrete C1 identifies the PMr2 as the best and the RPa1 as the worst. The deep scratches observed on the coupons suggest an abrasive-dominated wear mechanism with damages induced by the fines and granulates. The ranking is indeed correlated with the measured hardness from a previous work for PMr1 (12 ± 2 GPa), PMr2 (12 ± 2 GPa), and RPa1 (4.3 GPa) [40].

The concrete composition is important on the extent of damage. The concrete C2 induces less damage than the concrete C1 because the superplasticizer modifies the boundary layer and thus the interaction between the concrete particles and the liquid medium. Even though C2 is less aggressive and leaves metallic surfaces undamaged, its damaging ability is enough to impact the softer polymer. In all testing conditions, a threshold pressure below which no damage is induced by the concrete friction exists and is a function of the couple concrete-skin.

Table 3. Rating of formwork skin degradations after friction test according to the pressure and concrete. Rating is from 1 (not degraded) to 5 (very degraded).

Concrete	**C1**			**C2**			**Total rating**
Formwork skin	*60 kPa*	*80 kPa*	*110 kPa*	*60 kPa*	*80 kPa*	*110 kPa*	
PMr1	1	2	3	1	1	2	10
PMr2	1	2	2	1	1	1	8
RPa1	3	4	5	1	2	3	18

IV. Friction behavior

Figures 9 and 10 show the evolution of the dynamic friction stress as a function of contact pressure and concrete formulation for the three formwork skins. The linearity agrees with previous works on a concrete similar to C1 [3] for a contact pressure (50 to 110 kPa) below the threshold pressure evaluated at 120 kPa for a roughness Ra of 1.6µm [3][1] that is representative of our tested formwork skins. Above this pressure, the boundary liquid phase moves into the concrete volume and the surface adopts a granular behavior during shearing [18].

The friction stress increases with the contact pressure possibly because of an increase in intergranular contacts at the surface of the plate [27]. This stress causes part of the liquid phase and fines (of less than 80 µm diameter) to migrate towards the interface, resulting at the interface in the formation of a lubricating surface (or boundary) layer comprising water and fines. Both the concrete formulation and the skin material have a strong influence on the interfacial dynamic behavior.

For the concrete C1, significant differences are observed between the three formworks. The friction is smaller for PMr1 and greater for PMr2 with a friction coefficient twice greater. The C1 formulation has a more compact limit layer than C2 during compression. Consequently, the fines trapped in the asperities of the skins will be more important with this concrete. Consequently, the topography of the substrate should affect the friction of concrete when their limit layer is more compact. PMr2 has a roughness S_a, a real surface of contact S_{dr}, and volumes of asperities V_{vc} and valleys V_{vv} greater than PMr1 and RPa1. This means more concrete particles are trapped in the asperities of PMr2.

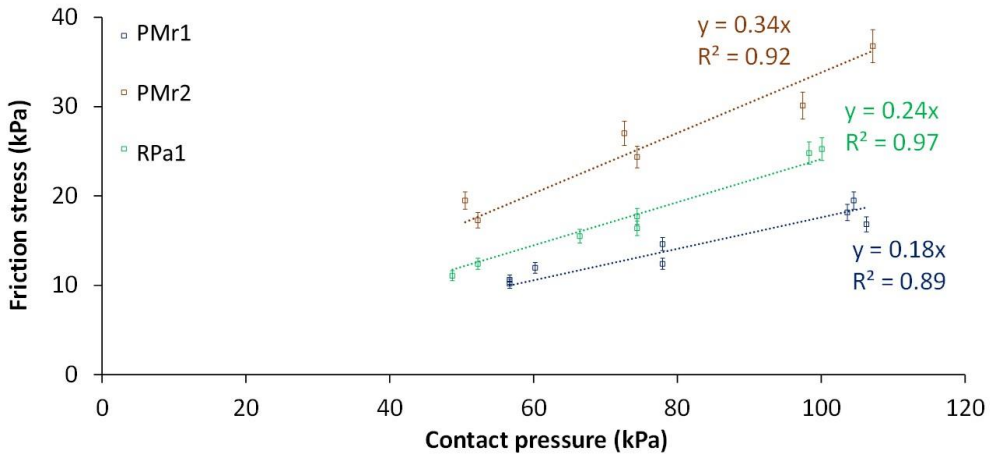

Figure 9. Evolution of the friction stress of C1 concrete as a function of contact pressure for each formwork skin.

The friction stress against C2 is varying linearly with normal pressure. The friction coefficients vary from 0.09 to 0.11. This value agrees with other similar works that found a range from 0.07 to 0.10 [3][31][30]. The friction is slightly higher for the polymer than metallic substrates.

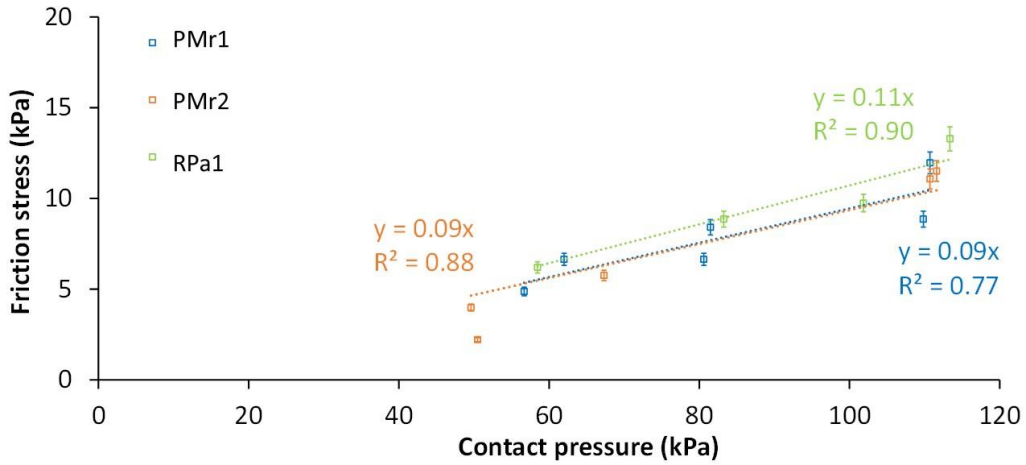

Figure 10. Evolution of the friction stress of C2 concrete as a function of contact pressure for each formwork skin.

The friction coefficient is proportional to the normal pressure applied by the concrete. This linear evolution corresponds to a Coulomb's law, in agreement with other works [2][3][31][26][30][29]. The linearity of the tangential force-normal pressure correlation indicates that the normal pressure (between 50 and 110 kPa) is always below the threshold pressure above which the liquid phase of the boundary layer rediffuses into the concrete bulk. At this stage, the surface behaves like a granular medium submitted to shear and a non-linear relationship between tangential and normal pressure is observed [1][27][18][30][55].

This result is proportional to the increase of intergranular contacts in the concrete that transmit the applied normal pressure to the formwork surface [1][27]. The concrete-to-surface friction coefficients are determined as the slope value of the fitting curves. The results are summarized in Table 4 and are in agreement with the values found in other works for fresh concrete on metallic plates with a R_a roughness value between 0.3 and 1.6 µm [24][2][27][28][31][29]. The constant value in friction coefficient for the investigated range of pressures indicates that the lubricated contact due to the presence of a water-containing boundary layer is always present [27].

Table 4. Dynamic friction coefficients of concrete/formwork skin interfaces in all configurations.

Formwork skin	Concrete	
	C1	*C2*
PMr1	0.18	0.09
PMr2	0.34	0.09
RPa1	0.21	0.11

E. Surface interactions in concrete/plate tribo-contacts

I. Interactions with C1

1. Effect of roughness

The interactions with the concrete C1 are strongly dependent on the substrates. The friction coefficient is the smallest for PMr1 and greatest for PMr2. A trend is evidenced in Figure 11 when plotting the skin roughness about the friction coefficient. The proportion of concrete particles able to be trapped in the asperities are calculated as the proportion of particles that have a diameter smaller than S_a according to the granulometry. The fitting relationship between the roughness parameter S_a (in µm) and the friction coefficient µ is given by:

$$\mu = 0.0625 \cdot S_a + 0.1138 \qquad (R^2=0.89) \qquad \text{(Eq. 6)}$$

Greater roughness induces greater friction because the peaks generate an energy dissipation though the rotation of the granulates [27][30]. Possible electrochemical binding effects are not considered because the duration of tribological testing (within the first ten minutes after pouring) is shorter than the kinetics of concrete curing and electrochemical interactions with the substrate (usually several hours).

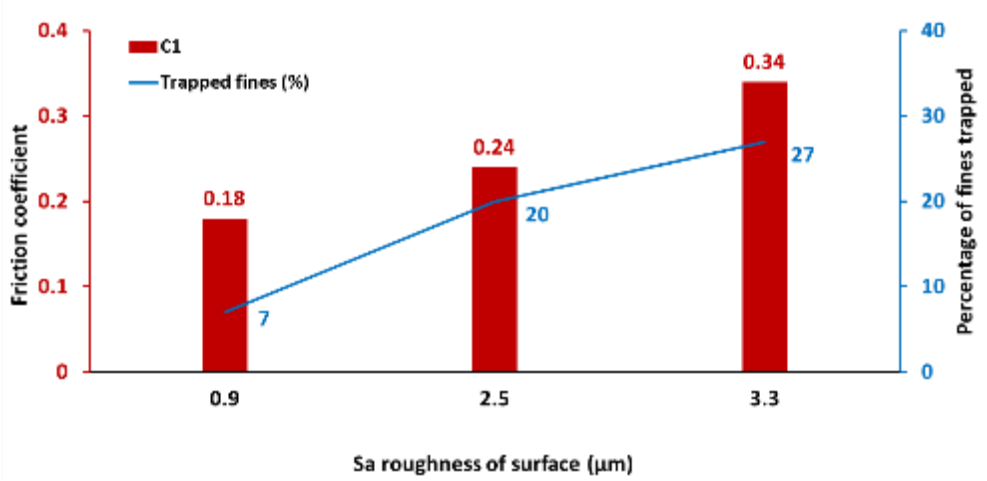

Figure 11. Histogram of coefficients of percentage of fines trapped and friction coefficient of C1 concrete for PMr1 (S_a = 0.9 µm), RPa1 (S_a = 2.5 µm) and PMr2 (S_a = 3.3 µm) substrates.

Another work investigated the friction of a concrete similar to C1 on a metallic plate with a roughness R_a of 1.7 µm [30][3]. Assuming an isotropic roughness along x and y, S_a should be related to R_a within 15% [56]. Thus, considering a S_a value between 1.4 and 2.0 µm, the predicted coefficient of friction with Eq. 1 is between 0.20 to 0.24 in agreement with the measured value of 0.21 from previous works [3].

2. Wear resistance

The wear resistance was quantified from optical interferometry measurements by using the changes in roughness parameters before and after tribological testing. When using the concrete formulation C1, a homogeneous wear of the peaks (running-in) occurs, forming plateaus in PMr2 (Figure 13), and is accompanied by deep scratches (up to 7 µm deep) parallel to the friction direction.

The applied normal pressure on the concrete forces the diffusion to the substrate surface of water and the finest particles (fines) [24] thus forming a concrete-substrate lubricant interface [2][27][31][29][55]. This effect referred to as the wall effect causes the large particles to push the smallest particles into the asperities [3][57] and is accompanied by a drop in solid content near the formwork surface [57][45]. The drop in solid content near the metallic surface is reduced for rough surfaces which traps the fines. The presence of water near the metallic surface implies a larger degree of freedom for cement particles than for clay particles [1][24].

The movement of fines above the surfaces induces a homogeneous uniform wear of the peaks which can lead to a drop in surface roughness of the coupon after testing (ploughing). This can be seen as some running-in effect. The concrete C1 is more compact than C2 leading to greater number of fines at the interface [1]. When shearing the boundary layer by displacing the coupon, the mechanical anchoring of the fines with the coupon asperities hinders the relative movement of the coupon in regard to the fresh concrete [27] leading to high friction coefficients.

When large granulates penetrate in the largest asperities of the formwork, the grains stemmed in the asperities generate large scratches when displaced into the material under the tangential forces [28]. This suggests that the flattening of the peaks results from the friction of the liquid medium containing the filler and cement particles while the deep scratches are formed by the large granulates.

The friction of C1 on RPa1 is damaging heavily the substrate even at small pressures (Figure 14) with scratches deeper than on metallic substrates. This agrees with higher damages for the polymer coating as its hardness is smaller than the hardness of the abrasive particles (granulates). Scratches show high pile-up along their sides (wedging). Some scratches revealed a complete removal of the coating leaving the substrate bare. The polymeric coating should thus be limited to only a few castings.

The metallic surfaces are not damaged for pressures below 80 kPa. Exceeding this pressure is sufficient for the granulates to create large scratches (Figures 12 and 13). Small traces of corrosion are visible on PMr1 after testing indicating that the penetration of granulates was deeper than the protective oxide layers.

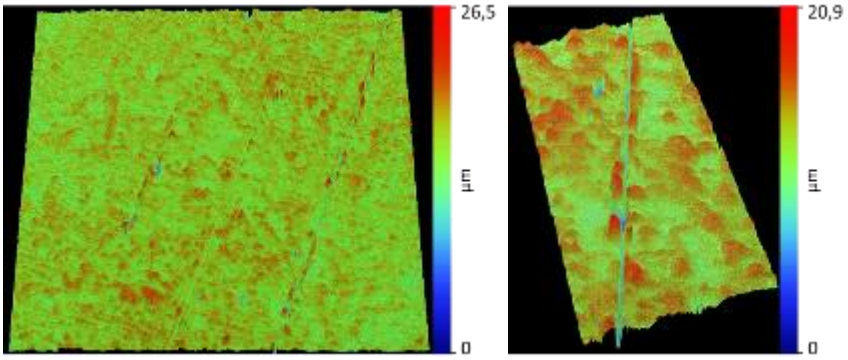

Figure 12. 3D cartography of PMr1 after friction of C1 concrete at 110 kPa: a) Overview and b) high magnification

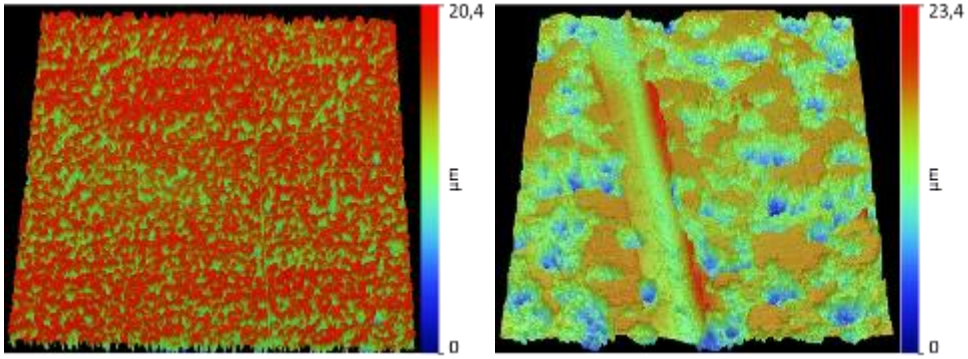

Figure 13. 3D cartography of PMr2 after friction of C1 concrete at 110 kPa: a) Overview and b) high magnification

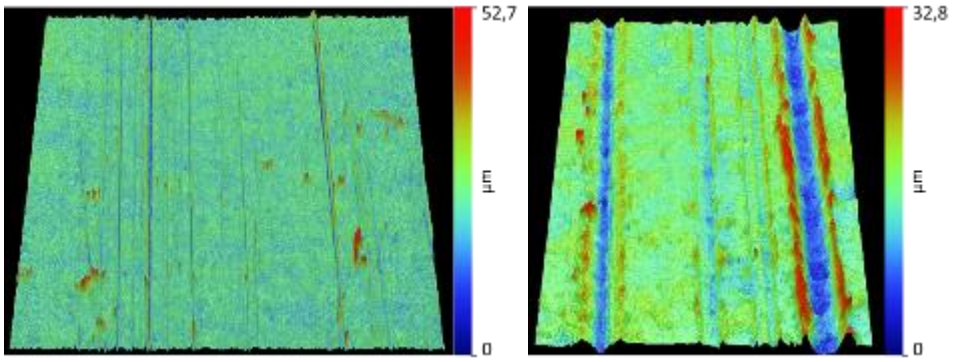

Figure 14. 3D cartography of RPa1 after friction of C1 concrete at 110 kPa: a) Overview and b) high magnification

3. Friction mechanisms

The abrasive wear results from the penetration and cutting of hard abrasive particles. The hard aggregates are believed to be at the origin of these large scratches. This may be due to a kinetic effect of the pressure transmission from aggregates to aggregates. These results highlight that the shear stress measured during a tribological test is the combined frictional effects of both the cement paste

and the local aggregates. On the other hand, the PMr2 formwork shows little damage from the concrete friction with only few small scratches at 110 kPa.

The model of Benjamin and Weaver [46] suggested an ultimate shear stress of 6.7 GPa for delamination of the oxide layer on the metallic substrate [40]. However, the normal stress of 110 kPa induced a friction stress of 20 kPa, 10^6 times less the one required to delaminate the oxide layer. Therefore, the large scratches seem to be due to a more intense, localized, granulate friction.

Scratch testing have identified the minimum pressure to leave an imprint using a 0.2 mm diameter, steel ball during sliding [40]. Assuming spherical granulate shapes spherical, the pressure P_0 on a disc surface of diameter d_0 is equal to the pressure P_1 exerted on a surface of diameter d_1 against the substrate:

$$p_0.\pi.\frac{{d_0}^2}{4} = p_1.\pi.\frac{{d_1}^2}{4} \quad \text{(Eq. 7)}$$

Considering as an approximate value of d_1 equal to the scratch width, Table 4 summarizes the ratio between d_0 and d_1 to leave a scratch of similar depth than observed at the threshold normal force for damaging during scratch test. This suggests that smaller granulates diameters should reduce the wear of the formworks, the crushed aggregates are the causes of the scratches, and the filler and cement particles are at the origin of peak wear. This simple calculation could be used to estimate the wear resistance of the substrates knowing the size of the granulates and the normal pressure of the fresh concrete on the formwork.

Table 4. Comparison between scratch test data (from [39]) and the diameter of aggregates d_1 to leave the same imprint at different normal pressures.

	Scratch testing (from [39]) (maximum values for ploughing mechanism before first critical point)			Diameter d_1 (in mm) to leave same imprint at different normal pressures		
material	Threshold force for damaging with 0.2 mm steel ball (N)	Scratch width (µm)	Average pressure (GPa)	60 kPa	80 kPa	110 kPa
PMr1	15N	55	6.3	18	15	13
PMr2	20N	55	8.4	21	18	15
RPa1	6N	112	0.6	11	10	8

II. Interactions with C2

The coupons submitted to the friction of C2 show smaller wear and friction coefficients than when sliding against C1. These two data suggest a change in the friction mechanism when adding superplasticizer to the concrete. Fresh concrete behaves as a thixotropic, non-Newtonian fluid [58][13][59]. The applied shear stress thus disperses the suspension of cement particles and water, leading to a drop in dynamic viscosity.

When the concrete is compressed, the migration of water and the fines near the formwork skin induces the formation of a boundary layer at the concrete-formwork interface. This migration is accompanied by a diffusion of the superplasticizer that induces the “deflocculation” of the fines in the close neighborhood of the formwork skin [3]. This phenomenon limits the compaction of the boundary layer

in comparison to the concrete without superplasticizer (Figure 15). Subsequently, during the sliding of the formwork, the boundary layer of the concrete containing superplasticizer undergoes a weaker internal shear and thus smaller friction stresses. The friction is mostly a lubricated friction when superplasticizer is added to concrete.

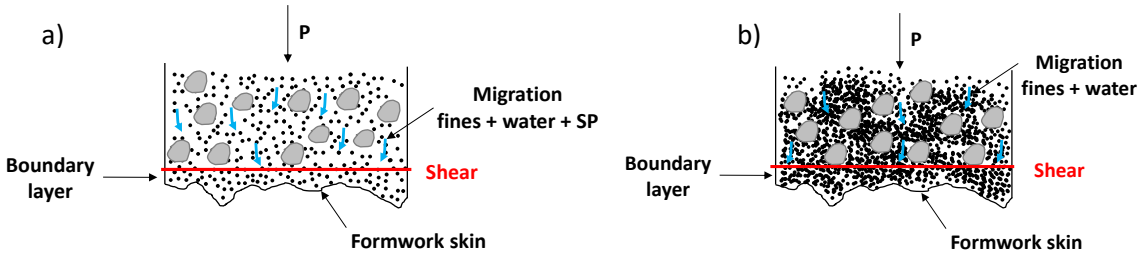

Figure 15. Schematics of concrete/formwork interfaces according to the concrete tested: a) C2, b) C1.

The roughness parameters do not vary significantly for all the formworks submitted to friction with a concrete containing superplasticizer. The scratch depth does not exceed 5 µm for PMr1 and 3µm for PMr2 with the contact pressure of 110 kPa. At 110 kPa, the polymer coating has scratches up to 30 µm depth highlighting its small resistance to scratching. This means that the addition of superplasticizer improves the fluidity of concrete for pouring easiness and lowers the friction and wear of the formwork, in agreement with other works [2].

The thicker boundary layer explains why the roughness of the plate does not impact significantly the friction coefficient. The mobility of a liquid in the interstices is high especially at small normal pressures. Recalling Eq. 1, it is interesting to note that, for a perfectly smooth surface (S_a = 0), the friction coefficient with C1 is 0.1138, similar to the one for the concrete C2 which is capillary dominated.

The slightly higher friction coefficient on RPa1 may be related to a higher water affinity as the friction coefficient drops for smaller solid surface energies of the substrate [60]. Data in Table 5 show a correlation between the coefficient of friction and the water affinity associated to greater capillary forces at the boundary layer. Thus, RPa1 has both a great affinity to water and a higher friction coefficient. Same conclusions are obtained with the drop in friction when adding vegetal oils [31] associated to the smaller wettability.

Table 5. Characterization of substrates from previous works with addition of friction coefficient

Material	Water contact angle (°) [39]	Free surface energy ($mN{\cdot}m^{-1}$) [41]	Work of adhesion ($mJ.m^{-2}$) [41]	Friction coefficient [Present work]
PMr1	104	38.7	55.6	0.09
PMr2	103	20.2	56.6	0.09
RPa1	71	15.6	96.4	0.11

F. DISCUSSION

I. Compare full-scale static friction to dynamic friction in laboratory

The friction of concrete on formworks during pouring is beneficial as it lowers the lateral pressure on the formworks thus reducing the dimensions of formworks design [3][1][4][61]. However, successive pouring induces a progressive wear of the formworks [27]. The comparison of the wear surfaces with full-scale testing of formworks remains difficult as the friction of the concrete against formworks is mostly static.

The same formwork material (PMr1, PMr2, RPa1) were analyzed from formworks used with a concrete similar to C1. PMr1 and PMr2 are analyzed after hundreds of castings while the polymeric coating is analyzed only after a few castings (Figures 16 and 17). The smaller lifespan of the RPa1 is in agreement with its weak resistance to the tribological test (Figure 18).

The PMr1 formwork shows after hundreds of castings grey spots of thin concrete residue and some red marks associated to corrosion products. The roughness increases after thousands of castings to 5.0 +/- 1.6 µm because of the high plateaus composed by the corrosion products. Another observation is the lack of long scratches. However, the corrosion product suggests that the concrete did indeed penetrate through the oxide layer at the surface. XRD analyses had proven that corrosion spots are a mixture of oxide-hydroxide FeO(OH) and $CaCO_3$, a product of the carbonation of calcium hydroxides $Ca(OH)_2$ [62]. These corrosion products are localized on spots where the protective oxide layers have been eliminated. Details are given in [39].

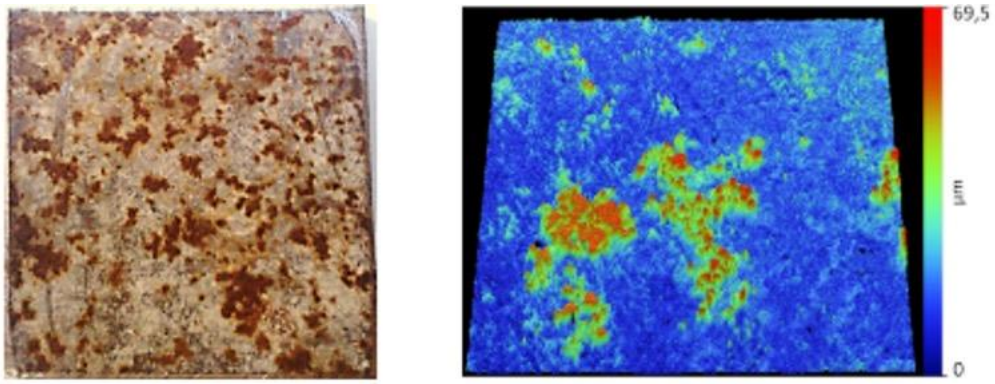

Figure 16. PMR1 formwork skin surface after full-scale testing: (a) Surface condition (50*50 mm^2) (b) 3D topography (8*8 mm^2).

The formwork of PMr2 reveals after hundreds of castings few small scratches and no corrosion product. The 3D topography shows a flattening of the plateau induced by the repetitive castings. Despite a drop of 30% of peak heights (confirming surface finishing effect), roughness has increased by 60% (S_a=4.6 µm) thus a wear less important than PMr1. The small damage on PMr2 confirms its good robustness observed during tribological testing. XRD reveals that the formwork did not change chemically during castings neither did it chemically react with concrete.

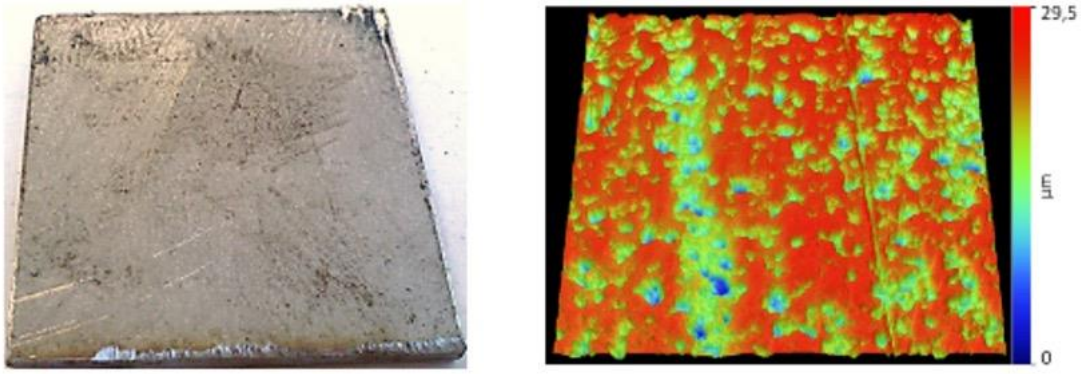

Figure 17. PMR2 formwork skin surface after full-scale testing: (a) Surface condition (50*50 mm^2) (b) 3D topography (8*8 mm^2)

The behavior is different for the polymer coating. The high damage after only tens castings agrees with tribological results and shows their little resistance to wear. It also agrees with the literature data and industry knowledge that these polymers are used only for a single or a small number of castings.

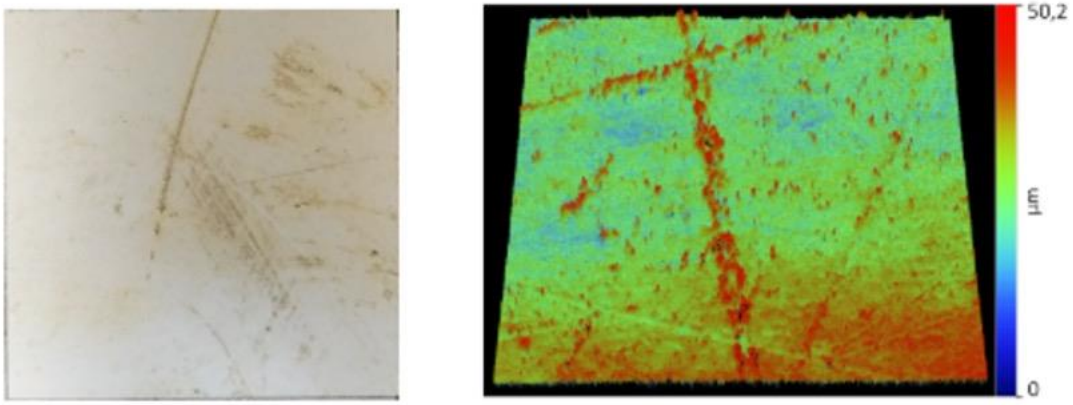

Figure 18. RPa1 formwork skin surface after full-scale testing: (a) Surface condition (50*50 mm^2) (b) 3D topography (8*8 mm^2)

These results show that the tribometer results agree qualitatively with full-scale observations and can be used to compare quickly different formwork materials. The authors believe that identifying the minimum normal pressure that creates defects is a good criterion to determine the lifespan of the formworks. However, the tribometer investigates only the wear actions of concrete but not the tribo-corrosion damages, a degradation process due to the combined effect of corrosion and wear. Sometime after testing, tribo-corrosion is visible as rusted spots similar to the formworks tested at full-scale.

II. Surface Topography Evolution

No significant change was observed when using the concrete C2, confirming that little wear occurs following the small friction coefficient. The lifespan of the formworks when using the concrete C2 is not an issue but adding superplasticizer can be expensive. Even though the minimum pressure can be

an indication of the lifespan, a coherent roughness parameter must be identified as representative of the wear.

Focusing on the concrete C1, among the numerous possible roughness parameters, the most pertinent in our study was the parameter V_{mp}. The friction being applied at the decimeter scale and the optical measurements at the millimeter and micrometer scales, this difference in scales leads to some scatter with correlation coefficients of 0.6 to 0.7. The V_{mp} volume parameter has been used to characterize the quantity of material which can be removed during a wear process of surface [63]. This explains why V_{mp} is an efficient indicator is a functional indicator of the wear magnitudes by granulates translation of formwork surfaces. This study reveals large scattering of the peak volumes V_{mp} at a given pressure after concrete friction. This is partially related to the difference in scales between the friction surface (100 cm^2) and the optical interferometric measurements (mm^2). Therefore, the authors consider a correlation coefficient R^2 of 0.6-0.7 to be significant. It is however clear that polymeric coatings are less resistant than metallic formworks.

No significant change of V_{mp} was observed for PMr2 (Figure 19) possibly due to an initial very high roughness which hides the wear process and the rare scratches that have been formed. The absence of correlation indicates a dominant homogeneous wear mechanism and little scratches formed. Even though the measurements have some dispersion, a general trend shows that the V_{mp} variation is usually positive and greater for high concrete pressures, as expected. For the formwork PMr2, there is no significant trend suggesting a small wear in the range of pressure. The negative variation reveals mostly a surface finishing effect and the erosion of the peaks of a rough surface initially with a Sa and peak height values of 3.3 and 9 µm, respectively. The variation of 10% is observed on the peak heights after friction. Some localized and isolated scratches of 7 µm depth can be observed.

RPa1 coatings deteriorate easily even at the smallest pressure of 60 kPa. The friction of concrete C2 on the polymeric coating RPa1 generate an increase in the peak volume (Vmp). The volume of peaks increases by 60% at 60 kPa up to 150 % at 110 kPa (Figure 20). This increase is explained by the formation of high pile-up along the scratch sides. The damage of the polymer is 10 times greater than the metallic surfaces with some scratches reaching 100 µm depth. This lack of resistance to wear of polymeric coating is correlated to its hardness 60 times smaller than the metallic formworks.

For PMr1 coupons, the roughness parameter V_{mp} is little affected (maximum of 25% in Figure 21), possibly due to initial low roughness and high hardness values. Nevertheless, some deep scratches of 15 µm-depths are observable on PMr1, induced by some of the large granulates but still smaller than the observed 102 µm-deep scratches on PP coatings. The drop in roughness parameter at small concrete pressure may possibly be due to the wear of the peaks without sufficient pressure for granulate-induced scratches. This kind of running-in phenomenon may explain the observed performing improvement of new steel formworks after some concrete castings. The negative variation of the roughness parameter below 75 kPa pressure (zone A) suggests a superficial wear of the top of the peaks and a pressure too small to induce a scratch at the surface. Indeed, no scratch is observed at 60 kPa. This surface finishing or break-in explains the observed improvement of the formwork efficiency after a few castings. At greater pressure than 75 kPa (zone B), the variations are positive up to +25% at 110 kPa, indicating more volumes in the peaks after friction. 3D topography measurement (recall Figures 16 to 18) after 110 kPa reveals the formation of pile-up induced by the scratch that

explain the increase in V_{mp}. Interferometry measurements also reveal that the scratches have a width always smaller than 70 µm suggesting that wear is induced by the fines and sand particles rather than the granulates of several mm in diameter. Moreover, the depth can exceed 15 µm, indicating a depth greater than the protective oxide coating. Oxidation marks are therefore observed at the locations deprived of their protective oxide layer after testing at a normal pressure of 110 kPa.

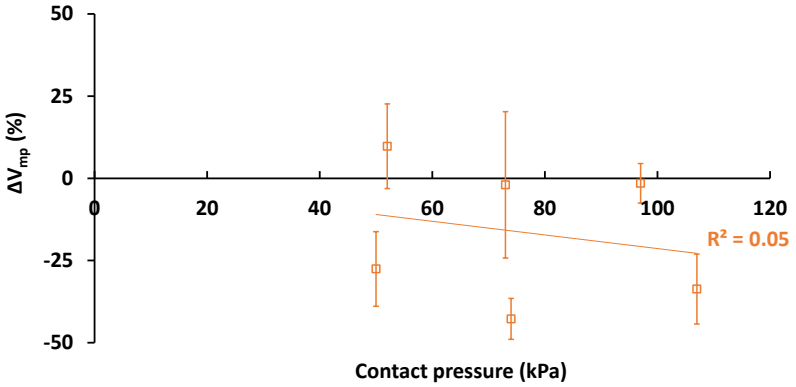

Figure 19. Variation of peaks material volume V_{mp} for the PMr2 skin according to the contact pressure after the friction of C1 concrete.

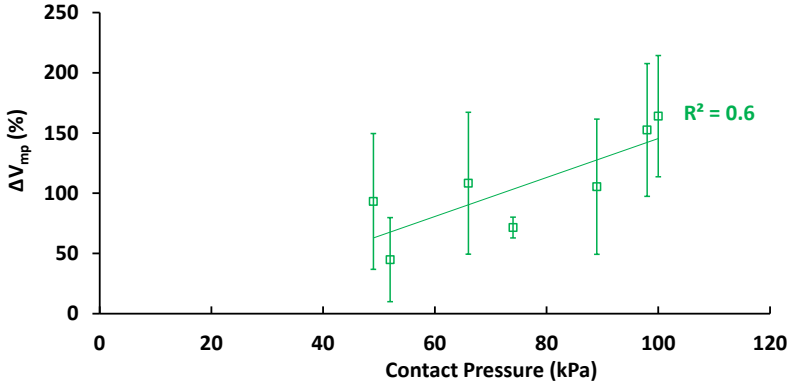

Figure 20. Variation of peaks material volume V_{mp} for the RPa1 according to the contact pressure after the friction of C1 concrete.

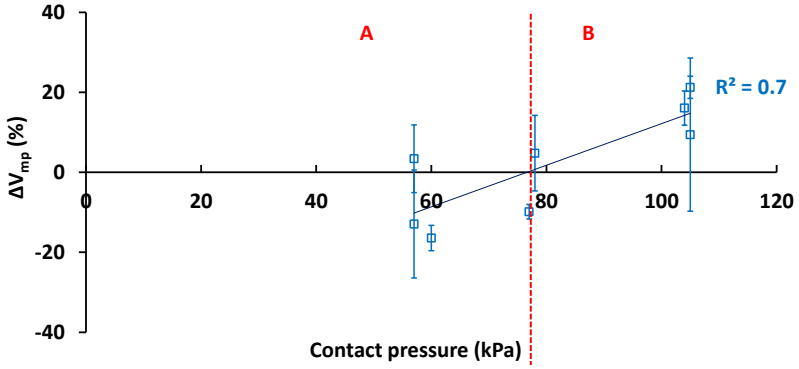

Figure 21. Variation of peaks material volume V_{mp} for the PMr1 skin according to the contact pressure after the friction of C1 concrete.

G. CONCLUSION

A laboratory-scale tribological test has been applied to evaluate the wear resistance of metal and polymer coupons for formwork applications. This test, which involves a controlled transverse travel speed of the coupon, successfully ranked the coupons regarding their wear resistance observed on full-scale testing. The wear resistance of the coupons was examined for different concrete pressures and formulations. Use was made of the roughness parameters to identify the wear resistance of the concrete-formwork system. In particular, the parameters S_a and V_{mp} in combination with the hardness and the surface tension of the substrates are regarded as suitable 3D surface analysis parameters for the surface tribological behavior against fresh concrete. Hard metallic surfaces are prone to running-in while softer skins are heavily damaged even at small normal pressures.

With a compact concrete (C1), mechanical anchoring dominates the tribological interfacial behavior. The friction coefficients of concrete with the coupons are related to the skin surface topography and the wear extent is correlated to the hardness. However, the friction coefficient and the degradation rate are not correlated. With a more fluid concrete (C2), capillary effects dominate the concrete/formwork interface during the concrete friction. A skin with a high free surface energy implies a better affinity with water and therefore a strong contact between the two components. A smaller damage with C2 is in agreement with a capillarity-dominated friction mode in comparison to a mechanical anchoring mechanism for C1. Indeed, in concretes containing superplasticizer, the inter-particle repulsion generates a less compact boundary layer at the interface with the substrate leading to a smaller friction stress.

Friction and wear results highlighted different underlying mechanisms at the concrete-formwork interfaces: either a shear stress in the liquid boundary layer or a granular friction from the concrete particles. First, the addition of superplasticizer to the concrete modifies the friction mode from mechanical anchoring- to capillarity-dominated. Second, the deterioration is induced by abrasive wear generated by both fines and granulates. Consequently, a formwork surface with high hardness and more peaks than valleys (that means high V_{mp}) should be selected to avoid deep scratches and favor running-in wear over scratch damaging. The local mechanisms, especially the migration of fines and water in the fresh concrete volume and the subsequent wear mode, are still partly hypothesized and must be supported by future experimental and modeling works.

H. ACKNOWLEDGEMENTS

The authors gratefully acknowledge the contribution of our colleagues S. Mezghani and A. Montagne from Arts et Métiers ParisTech, and Y. Vanhove from Génie Civil et de géo-Environnement laboratory (LGCgE) for their technical support.

I. REFERENCES

[1] Y. Vanhove, Contribution à l'étude du frottement d'un béton autoplaçant contre une surface métallique - Application aux poussées contre les coffrages, Thèse Dr. Univ. d'Artois. (2001).

[2] S. Bouharoun, P. De Caro, I. Dubois, C. Djelal, Y. Vanhove, Effect of a superplasticizer on the properties of the concrete / oil / formwork interface, Constr. Build. Mater. 47 (2013) 1137–1144. https://doi.org/10.1016/j.conbuildmat.2013.05.029.

[3] S. Bouharoun, Comportement tribologique des huiles de décoffrage à l ' interface béton / coffrage - Influence de la formulation du béton, (2011).

[4] K. El Cheikh, Étude de l'interface milieu granulaire – paroi rugueuse par approches expérimentale et numérique – Application aux bétons, Université d'Artois et Ecole nationale supérieure des Mines Douai, 2015.

[5] Y. Vanhove, C. Djelal, A. Magnin, Prediction of the lateral pressure exerted by self-compacting concrete on formwork, Mag. Concr. Res. 56 (2004) 55–62. https://doi.org/10.1680/macr.2004.56.1.55.

[6] P. De Caro, C. Djelal, L. Libessart, I. Dubois, Influence of the nature of the demoulding agent on the properties of the formwork-concrete interface, Mag. Concr. Res. 59 (2007) 141–149. https://doi.org/10.1680/macr.2007.59.2.141.

[7] K. El Cheikh, S. Rémond, P. Pizette, Y. Vanhove, C. Djelal, Discrete Element study of granular material - Bumpy wall interface behavior, Phys. A Stat. Mech. Its Appl. 457 (2016) 526–539. https://doi.org/10.1016/j.physa.2016.03.053.

[8] J.-M. Georges, Frottement, usure et lubrification, la tribologie ou science des surfaces, in: CNRS Editi, 2000.

[9] T.T. Ngo, E.H. Kadri, R. Bennacer, F. Cussigh, Use of tribometer to estimate interface friction and concrete boundary layer composition during the fluid concrete pumping, Constr. Build. Mater. 24 (2010) 1253–1261. https://doi.org/10.1016/j.conbuildmat.2009.12.010.

[10] D. Feys, K.H. Khayat, A. Perez-Schell, R. Khatib, Development of a tribometer to characterize lubrication layer properties of self-consolidating concrete, Cem. Concr. Compos. 54 (2014) 40–52. https://doi.org/10.1016/j.cemconcomp.2014.05.008.

[11] G.C. Cordeiro, L.M.S.C. De Alvarenga, C.A.A. Rocha, Rheological and mechanical properties of concrete containing crushed granite fine aggregate, Constr. Build. Mater. 111 (2016) 766–773. https://doi.org/10.1016/j.conbuildmat.2016.02.178.

[12] J.-F. Wallevik, Computational rheology, thixotropy explorations of cement pastes; An introduction, in: 3rd Int. Symp. Self-Consolidating Concr., Reykjavik, Iceland, 2003.

[13] J.E. Wallevik, Thixotropic investigation on cement paste: Experimental and numerical approach, J. Nonnewton. Fluid Mech. 132 (2005) 86–99. https://doi.org/10.1016/j.jnnfm.2005.10.007.

[14] G.H. Tattersall, The rhéology of fresh concrete, Pitman Adv, 1983.

[15] F. De Larrard, C.F. Ferraris, T. Sedran, Fresh concrete: A Herschel-Bulkley material, Mater. Struct. Constr. 31 (1996) 494–498. https://doi.org/10.1007/bf02480474.

[16] C.-F. Ferraris, F. De Larrard, Testing and modelling of fresh concrete rheology, NISTIR 6094. (1998).

[17] C.-F. Ferraris, Measurement of the rheological properties of high performance concrete: state of the art, J Res Natl Inst Stand Technol. 15 (1999) 104.

[18] Y. Vanhove, C. Djelal, A. Magnin, A device for studying fresh concrete friction, Cem. Concr. Aggregates. 26 (2004) 35–41. https://doi.org/10.1520/cca11897.

[19] Bleschik, Les propriétés mécaniques et la rhéologie des bétons, Minsk, 1977.

[20] Y. Tanigawa, H. Mori, K. Tsutsui, Y. Kurokawa, Constitutive law and yield condition of fresh

concrete, Trans. Japan Concr. Inst. 9 (1987) 47–50.

[21] H. Fujiwara, S. Nagataki, Study on self-compactability of high-fluidity concrete, in: Self-Compacting Concr., Stockholm, 1999.

[22] T. Proske, Frischbetondruck bei Verwendung von Selbstverdichtendem Beton - Ein wirklichkeitsnahes Modell zur Bestimmung der Einwirkungen auf Schalung und Rüstung, Beton- und Stahlbetonbau. 104 (2009) 88–96.

[23] S.H. Kwon, Q.T. Phung, H.Y. Park, J.H. Kim, S.P. Shah, Experimental study on effect of wall friction on formwork pressure of self-consolidating concrete, in: 6th Int. RILEM Symp. Self-Compacting Concr. 4th North Am. Conf. Des. Use SCC, 2010.

[24] C. Djelal, Designing and perfecting a tribometer for the study of friction of a concentrated clay-water mixture against a metallic surface, Mater. Struct. 34 (2001) 51–58.

[25] C. Beaumel, Extrusion des pâtes d'argile, Univ. Grenoble, 1998.

[26] S. Bouharoun, Y. Vanhove, C. Djelal, P. De Caro, I. Dubois, Interactions between Superplasticizer and Release Agents at the Concrete / Formwork Interface, Mater. Sci. Appl. 3 (2012) 384–389.

[27] C. Djelal, Y. Vanhove, A. Magnin, Tribological behaviour of self compacting concrete, Cem. Concr. Res. 34 (2004) 821–828. https://doi.org/10.1016/j.cemconres.2003.09.013.

[28] Y. Vanhove, C. Djelal, Friction mechanisms of fresh concrete under pressure, Int. J. Chem. Eng. Technol. 4 (2013) 67–81.

[29] S. Bouharoun, Friction behaviour of fresh concrete in the vicinity of formwork, J. South African Inst. Civ. Eng. 55 (2013) 10–17.

[30] C. Djelal, Y. Vanhove, L. Libessart, Analysis of friction and lubrication conditions of concrete / formwork interfaces, Int. J. Civ. Eng. Technol. 7 (2016) 18–30.

[31] C. Djelal, P. de Caro, L. Libessart, I. Dubois, N. Pébère, Comprehension of demoulding mechanisms at the formwork / oil / concrete interface, Mater. Struct. 41 (2008) 571–581. https://doi.org/10.1617/s11527-007-9268-3.

[32] K. El Cheikh, C. Djelal, Y. Vanhove, P. Pizette, S. Remond, Experimental and numerical study of granular medium-rough wall interface friction, Adv. Powder Technol. 29 (2018) 130–141.

[33] Y. Vanhove, C. Djelal, T. Chartier, Ultrasonic wave reflection approach to evaluation of fresh concrete friction, J. Adv. Concr. Technol. 6 (2008) 253–260. https://doi.org/10.3151/jact.6.253.

[34] P.H. Billberg, N. Roussel, S. Amziane, M. Beitzel, G. Charitou, B. Freund, Field validation of models for predicting lateral form pressure exerted by SCC, Cem. Concr. Compos. 54 (2014) 70–79.

[35] N. Roussel, G. Ovarlez, A physical model for the prediction of pressure profiles in a formwork, in: 2nd North Am. Conf. Des. Use Self-Consolidating Concr. (SCC 2005), 4th Int. RILEM Symp. Self-Compacting, 2005.

[36] G. Ovarlez, N. Roussel, A physical model for the prediction of lateral stress exerted by self-compacting concrete on formwork, Mater. Struct. 39 (2006) 269–279.

[37] C.A. Graubner, T. Proske, Formwork pressure: A new concept for the calculation, in: Proc. 2nd North Am. Conf. Des. Use Self-Consolidating Concr. (SCC 2005) 4th Int. RILEM Symp. Self-Compacting Concr., Northwestern Univ., Evanston, IL., 2005: p. 2005.

[38] C. Chadfeau, Caractérisations multiéchelles de surfaces cimentaires de parement en fonction de différentes surfaces coffrantes, Univ. Strasbourg, 2020.

[39] N. Spitz, Développement d'un procédé frugal de démoulage in-situ des parois de coffrage -

Etude des signatures fonctionnelles des parois de coffrage, 2019.

[40] N. Spitz, N. Coniglio, M. El Mansori, A. Montagne, S. Mezghani, On functional signatures of bare and coated formwork skin surfaces, Constr. Build. Mater. 189 (2018) 560–567.

[41] N. Spitz, N. Coniglio, M. El Mansori, A. Montagne, S. Mezghani, Quantitative and representative adherence assessment of coated and uncoated concrete-formwork, Surf. Coatings Technol. 352 (2018) 247–256. https://doi.org/10.1016/j.surfcoat.2018.07.098.

[42] K.J. Chin, H. Zaidi, T. Mathia, Oxide film formation in magnetized sliding steel/steel contact - Analysis of the contact stress field and film failure mode, Wear. 259 (2005) 477–481. https://doi.org/10.1016/j.wear.2005.02.122.

[43] C. Vergne, C. Boher, R. Gras, C. Levaillant, Influence of oxides on friction in hot rolling: Experimental investigations and tribological modelling, Wear. 260 (2006) 957–975. https://doi.org/10.1016/j.wear.2005.06.005.

[44] X. Yu, Z. Jiang, D. Wei, C. Zhou, Q. Huang, D. Yang, Tribological properties of magnetite precipitate from oxide scale in hot-rolled microalloyed steel, Wear. 302 (2013) 1286–1294. https://doi.org/10.1016/j.wear.2013.01.015.

[45] P. Coussot, C. Ancey, Rhéophysique des pâtes et des suspensions, 1999.

[46] P. Benjamin, C. Weaver, Measurement of adhesion of thin films, Proc. R. Soc. London. Ser. A. Math. Phys. Sci. 254 (1960) 163–176. https://doi.org/10.1098/rspa.1960.0012.

[47] AFNOR, NF P 18-404 Essai d'étude, de convenance, et de contrôle - Confection et conservation des éprouvettes, 1981.

[48] AFNOR, NF EN 12350 Essai pour béton frais, 2009.

[49] AFNOR, NF EN 206 Béton - Spécifications, performances, production, et conformité, 2014.

[50] N. Coniglio, N. Spitz, M. El Mansori, Designing metallic surfaces in contact with hardening fresh concrete: A review, Constr. Build. Mater. 255 (2020) 119384. https://doi.org/10.1016/j.conbuildmat.2020.119384.

[51] S. Mezghani, Approches multi-échelles de caractérisation tridimensionnelle des surfaces, Arts et Métiers ParisTech, 2005.

[52] H. Zahouani, S. Mezghani, R. Vargiolu, M. Dursapt, Identification of manufacturing signature by 2D wavelet decomposition, Wear. 264 (2008) 480–485. https://doi.org/10.1016/j.wear.2006.08.047.

[53] AFNOR, Spécification géométrique des produits (GPS) - État de surface : surfacique - Partie 2 : termes, définitions et paramètres d'états de surface, 2012.

[54] AFNOR, Spécification géométrique des produits (GPS) - État de surface : surfacique - Partie 3 : opérateurs de spécification, 2012.

[55] C. Djelal, Y. Vanhove, P. De Caro, A. Magnin, Role of demoulding agents during self-compacting concrete casting in formwork, Mater. Struct. 35 (2002) 470–476.

[56] H.T. Lancashire, A simulated comparison between profile and areal surface parameters: Ra as an estimate of Sa, ArXiv. (2017) 1–9. http://arxiv.org/abs/1708.02284.

[57] Y. Vanhove, C. Djelal, G. Schwendenmann, P. Brisset, Study of self consolidating concretes stability during their placement, Constr. Build. Mater. 35 (2012) 101–108. https://doi.org/10.1016/j.conbuildmat.2012.02.019.

[58] P.F.G. Banfill, The rheology of fresh mortar, Mag. Concr. Res. 43 (1991) 13–21. https://doi.org/10.1680/macr.1991.43.154.13.

[59] C. Ferraris, F. Larrard, N. Martys, Fresh concrete rheology: recent developments, Mater. Sci. Concr. VI (2001) 215–241.

[60] M. Cartier, P. Kapsa, Usure des contacts mécaniques - Elements de tribologie, Tech. l'ingénieur. BM5066 (2001) 1–15.

[61] A. Zeitschrift, P. Link, E. Dienst, E. Eth, Pression du béton frais sur les coffrages, Bull. Du Cim. 27 (1959). https://doi.org/10.5169/seals-145523.

[62] C. Ployaert, La Corrosion des armatures des bétons armés et précontraints, Fédération de l'Industrie Cimentière Belge. (2008) 15.

[63] R. Leach, Characterisation of areal surface texture, 2013. https://doi.org/10.1007/978-3-642-36458-7.